Sustainable Cities and Society 76 (2022) 103376

Contents lists available at ScienceDirect

Sustainable Cities and Society

journal homepage: www.elsevier.com/locate/scs

A quasi-experimental approach for evaluating the heat mitigation effects of green roofs in Chicago, Illinois

Kathryn McConnell [a,*], Christian V. Braneon [b,c,*], Equisha Glenn [b,d], Natasha Stamler [e], Evan Mallen [f], Daniel P. Johnson [g], Raaghav Pandya [h], Jacob Abramowitz [i], Gabriel Fernandez [j], Cynthia Rosenzweig [k,b]

[a] School of the Environment, Yale University, 195 Prospect Street, New Haven, CT 06511, USA
[b] NASA Goddard Institute for Space Studies, 2880 Broadway, New York, NY 10025, USA
[c] SciSpace LLC, 6550 Rock Spring Drive, Suite 600, Bethesda, MD 20817, USA
[d] The City College of the City University of New York, 160 Convent Ave, New York, NY 10031, USA
[e] Massachusetts Institute of Technology, 77 Massachusetts Avenue, Cambridge, MA 02139, USA
[f] Georgia Institute of Technology, College of Design, 245 Fourth Street NW, Atlanta, GA 30332, USA
[g] Indiana University, 425 University Boulevard, Indianapolis, IN 46202, USA
[h] Columbia University Teachers College, 525 West 120th Street, New York, NY 10027, USA
[i] The University of Alabama in Huntsville, 301 Sparkman Drive, Huntsville, AL 35899, USA
[j] Columbia University, 1130 Amsterdam Avenue, New York, NY 10027, USA
[k] Center for Climate Systems Research, Earth Institute, Columbia University, 2880 Broadway, New York, NY 10025, USA

ARTICLE INFO

Keywords:
Green roofs
Green infrastructure
Urban Heat Island
Heat mitigation
Land surface temperature
Climate change adaptation
Remote sensing

ABSTRACT

In the coming decades, millions of urban residents will be exposed to increasingly deadly heat extremes. As an adaptive response to rising temperatures, many cities have begun to install vegetated "green" roofs, which now vary widely in structure and size, and have generally been shown to have cooling capacity. Yet, little research has been done to differentiate which types of green roofs are most effective at reducing urban heat. We present a method to evaluate the cooling effects associated with green infrastructure that draws on publicly available satellite imagery and open-source software for analysis. Based on a quasi-experimental research design that integrates social and physical science approaches, this technique is able to identify the cooling effects of green infrastructure against background warming trends associated with urbanization and climate change. We demonstrate this method at three green roof sites across the City of Chicago, finding that the study sites with larger, intensive green roofs accompanied by diverse plant species have greater cooling benefits than the extensive, monoculture green roof. Our low-cost method can aid policymakers and planners in empirically evaluating the cooling capacity of green roofs in their own communities.

1. Introduction

The growth of urban populations and expansion of urban land cover alongside rising global temperatures mean that millions of people will be exposed to potentially deadly urban heat in the coming century (Hoegh-Guldberg et al., 2018). Green infrastructure projects – such as vegetated roofs, greenspaces, street trees, and vertical greenery – are a critical means of adapting to these rising temperatures (Bowler, Buyung-Ali, Knight, & Pullin, 2010; Gill, Handley, Ennos, & Pauleit, 2007), and are now widely advanced as a heat mitigation strategy by researchers, urban planners, and policymakers (Norton et al., 2015; Zhang, He, & Dewancker, 2020). Yet, there is still a limited scholarly understanding of which types of green infrastructure are most effective at reducing urban heat (Bartesaghi Koc, Osmond, & Peters, 2018), and whether their heat mitigation performance varies across climatic regions. Given that local governments often have limited city budgets for climate planning (Aylett, 2015), comparative research that evaluates the relative effectiveness of different types of green infrastructure projects can provide pragmatic guidance for planners working on the ground.

Since at least the 1960s, vegetated or "green" roofs have been advanced as a key form of green infrastructure that can reduce building energy use and urban heat (Oberndorfer et al., 2007; Shafique, Kim, & Rafiq, 2018). As green roofs have spread, the term itself has come to encompass a diverse assortment of vegetated roof types that vary in

* Corresponding authors.
E-mail addresses: kathryn.mcconnell@yale.edu (K. McConnell), christian.v.braneon@nasa.gov (C.V. Braneon).

https://doi.org/10.1016/j.scs.2021.103376
Received 9 July 2021; Received in revised form 26 August 2021; Accepted 17 September 2021
Available online 25 September 2021

plant and substrate type, species diversity, size, and upkeep. Broadly, green roofs can be categorized as either "intensive" or "extensive", with intensive roofs being characterized by a variety of shrubs, trees, and other herbaceous plants requiring deeper soil and irrigation. Extensive roofs tend to have shallower soil and host low-lying plants such as *Sedum* species, which require little to no irrigation (Heusinger & Weber, 2017; Zheng et al., 2021). Limited experimental research suggests that these characteristics can all affect the cooling capacity of a given green roof (Blanusa et al., 2013; MacIvor & Lundholm, 2011). Given the wide range of green roofs available, more detailed, comparative evaluations of green roof impacts are needed to aid decision-makers in selecting the optimal roof type for their site (Mahdiyar, Tabatabaee, Abdullah, & Marto, 2018).

Utilizing publicly accessible Landsat 5 satellite imagery and open-source software, we demonstrate a low-cost technique for evaluating the heat mitigation performance of vegetated rooftops. We apply this analysis technique to three distinct vegetated roofs within the City of Chicago, intentionally selecting both intensive and extensive study sites that differed in their plant types, size, and location. This case comparison demonstrates the heterogeneity in green roof cooling performance – even among a sample of only three rooftops – emphasizing the need for more focused efforts to determine which types of green roofs offer the greatest cooling benefits and which can fully offset broader warming trends associated with climate change and urban densification.

1.1. Urban heat

In the coming century, heat waves are projected to grow in intensity, frequency, and duration, and to have the most pronounced impacts in urban areas (Habeeb, Vargo, & Stone, 2015; Meehl & Tebaldi, 2004). Known as the Urban Heat Island (UHI), urbanization's simultaneous expansion of impermeable surfaces and anthropogenic heat emissions often results in higher temperatures within cities compared to outlying rural or suburban regions (Mohajerani, Bakaric, & Jeffrey-Bailey, 2017). The UHI is driven by urbanization's reduction in vegetation levels and changes to surface geometries, which in turn reduce evapotranspiration (Chapman, Watson, Salazar, Thatcher, & McAlpine, 2017; Oke, 1982). Further, as urban areas grow denser, buildings, vehicles, and humans all emit their own sources of heat (Allen, Lindberg, & Grimmond, 2011). Thus, the intensity of UHI is closely linked to land use characteristics, in which denser development tends to correspond with higher intensity UHI (Chapman et al., 2017; Erdem Okumus & Terzi, 2021; Guo et al., 2020; Halder, Bandyopadhyay, & Banik, 2021). While the presence of vegetated green spaces within urban areas tends to mitigate the UHI (Liu, Zhang, Zhang, Zhang, & Teng, 2021), projections suggest that they cannot always outweigh the heating effects of building densification (Tian et al., 2021).

Climate change impacts dynamically interact with the UHI, in some future projections actually reducing future nighttime temperatures (Krayenhoff, Moustaoui, Broadbent, Gupta, & Georgescu, 2018; Oleson, 2012), but in many cases exacerbating heat stress. An emerging line of research suggests that heat waves can interact with and amplify existing UHI conditions, resulting in higher impacts in urban areas (Rizvi, Alam, & Iqbal, 2019; Tewari et al., 2019). For example, during heat waves in Shanghai, resulting changes in wind direction blew in warmer air from neighboring cities instead of the usual cooling sea breeze (Jiang, Lee, Wang, & Wang, 2019). Scholars anticipate a 700% increase in the number of urban dwellers regularly exposed to extreme heat by 2050 (Urban Climate Change Research Network, 2018), projecting that more than 35% of the world's population would be exposed to regular heat waves under a 2 °C warming scenario (Dosio, Mentaschi, Fischer, & Wyser, 2018).

As one of the largest drivers of weather-related mortality (Oleson et al., 2015), heat stress is already a major health concern around the world. Beyond deaths, extreme heat has also been linked to adverse respiratory and cardiovascular outcomes, as well as increased pollutant concentrations and their attendant health effects (Santamouris, 2015). Such impacts in turn tend to disproportionately impact socially vulnerable groups, such as the elderly and people living in poverty (Basu, 2009). In addition to health effects, temperature spikes have also been associated with reduced economic growth, as well as lower agricultural and industrial production (Dell, Jones, & Olken, 2012). Given these known impacts of extreme heat, projected increases in heat waves pose major threats to the health and wellbeing of millions of people around the world.

1.2. Green infrastructure for heat mitigation in Chicago

In 1995, Chicago experienced one of the deadliest and most widely-publicized heat waves in recent history, resulting in more than 700 deaths (Klinenberg, 2015). While this particular heat wave stands out as especially lethal, climate change projections suggest that it may not be an anomalous event; in fact, both average and extreme temperatures are predicted to increase in Chicago, as are the frequency and intensity of heat waves (Hayhoe, Sheridan, Kalkstein, & Greene, 2010).

In response to the 1995 heat wave and the prospect of intensifying urban heat, the City of Chicago adopted a range of green infrastructure interventions that aim to cool the city. These efforts have included development incentives for vegetated roofs (Chicago Zoning Ordinance, 2015; Kazmierczak & Carter, 2010) and zoning requirements for reflective roof implementation on new buildings (Chin et al., 2008). Thanks to these policies, Chicago has become a leading city in green and reflective roof implementation and is a valuable laboratory for better understanding the long-term effects of green infrastructure on urban heat (Smith & Roebber, 2011).

As a leader in incentivizing green roof development, Chicago has been the focus of a number of green roof case studies. Sharma et al. (2016), Smith and Roebber (2011) utilize the Weather Research and Forecasting models to simulate rooftop temperatures for various cool roof scenarios while Coseo and Larsen (2014) draw on air temperature measurements to investigate the urban heat across eight different neighborhoods (Coseo & Larsen, 2014; Sharma et al., 2016; Smith & Roebber, 2011). Such ground-based measurements and predictive modeling approaches are complemented by the use of satellite imagery (Hurwitz, Braneon, Kirschbaum, Mandarino, & Mansour, 2020), which provides extensive spatial coverage coupled with the ability to analyze changes over many years (Li et al., 2013; Yuan & Bauer, 2007). We build on these efforts, such as Mackey, Lee, and Smith's (2012) analysis of green and white roofs and Wilson and Chakraborty's (2018) vulnerability mapping across Chicago (Mackey et al., 2012; Wilson & Chakraborty, 2018).

1.3. Methods for evaluating Green roof heat mitigation effectiveness

Researchers have concluded that green roofs generally reduce urban heat (Berardi, 2016). Yet tradeoffs between accessible data and the robustness of various analytical methods have meant that there is limited research further qualifying this finding, which is critical for guiding practitioners in selecting the green roof types that offer maximal cooling benefits. For example, nearly 70% of research on green infrastructure utilizes observational methods (Bartesaghi Koc et al., 2018), often drawing on measurements from monitoring units (Zheng et al., 2021) or remote sensing time series data (Dong et al., 2020). While the use of longitudinal remote sensing imagery allows researchers to exploit publicly available data with global geographic and multi-decadal temporal coverage, Bartesaghi Koc et al. (2018) note that such observational research is often analytically limited to analyzing simple linear correlations (Bartesaghi Koc et al., 2018). This type of methodological approach makes it difficult to rigorously attribute changes in temperature to a vegetated roof from other concurrent changes to the local environment, and has recently been called into question as an effective technique (Parison, Hendel, & Royon, 2020).

In contrast, experimental studies allow the researcher to carefully control for external influences, isolating the causal effects of the green infrastructure project in question. While analytically more robust, such studies tend to rely on measurements collected via ground monitoring networks, which can be cost-intensive, limited in their geographic and temporal coverage, and difficult to replicate (Bartesaghi Koc et al., 2018). As a result, such studies are still relatively limited (Mallen, Bakin, Stone, Sivakumar, & Lanza, 2020).

While literature on green infrastructure tends to describe observational and experimental research designs as mutually exclusive, the two approaches can be blended. We utilize such a method through a quasi-experimental research design, which applies an experimental framework to observational data, effectively gaining the data availability and analytical benefits of both approaches. We argue that this approach offers a methodological improvement over much existing literature on green infrastructure's heat mitigation capacity for several reasons.

First, studies that analyze changes in land cover and urban heat with remote sensing data often rely on a small number of paired scenes, calculating the change over time between a single image (or just a few images) taken from an initial time frame and a second image (or just a few images) taken from a more recent time frame (Chen, Zhao, Li, & Yin, 2006; Dong et al., 2020; Gohain, Mohammad, & Goswami, 2021). For example, Mackey et al. (2012) analyze the effects of green infrastructure by calculating the change in surface temperature between five image pairs (constructed from eight total images) (Mackey et al., 2012). This approach results in a relatively small number of sample points for subsequent statistical analysis, limiting the robustness of results. In an attempt to increase the number of sample points available for analysis, the following study draws on a longer timescale of data and a larger number of satellite scenes – between 32 and 55 for each site, taken from between 1989 and 2011. This time frame allows for analyses with at least 15 scenes before and 17 scenes after the date of vegetated roof installation (see Table 1). Additionally, we only utilize data from Landsat 5 TM, avoiding any potential introduction of bias associated with differences between Landsat instruments.

Second, longitudinal analyses that only calculate change over time at the intervention site are limited in their ability to make robust causal inferences. This approach assumes that the intervention itself – in our case, the installation of a green roof – is the *only* change taking place that could cause subsequent changes in outcome variables, which in our case are land surface temperature (LST) and normalized difference vegetation index (NDVI), a measure of vegetation health (Smith, 2002). However it is almost never the case that extraneous variables remain unchanged in a multi-year observational setting, so the ability to isolate the effect of the green roof alone becomes critical. We calculate the causal effect of green roofs on urban heat and vegetation by evaluating LST and NDVI before and after green roof installation, at both the green roof site itself (referred to as the "treatment" site) and at a nearby rooftop without any green infrastructure (referred to as the "control" site). The causal effect of the green roof is ultimately evaluated by analyzing the change over time in LST at the treatment site *relative to the control site*. This difference-in-differences analysis allows us to identify the effects of the green roof from among other environmental changes which may influence both the treatment and control site. Used widely in fully experimental settings and for program evaluation, this research design was also proposed recently as an improved method for quantifying the impacts of green infrastructure on urban heat (Parison et al., 2020).

2. Materials and methods

2.1. Study sites

This study draws on Landsat 5 TM imagery to evaluate the effects of three vegetated rooftops in the City of Chicago on vegetation levels and land surface temperature over time. The three selected sites are a Walmart Supercenter rooftop, Millennium Park, and City Hall's rooftop, all of which are distinct in their form and human use. By modeling NDVI and LST on each rooftop over the course of 12 to 23 summers, we are able to evaluate whether the installation of vegetation resulted in significant changes in urban heat.

2.1.1. Millennium Park

Completed in 2004 after six years of construction, Millennium Park covers 99,000 m^2, making it one of the largest green roofs in the world. It was financed by the City of Chicago and private donors to cover parking garages and the Illinois Central Railroad rail yard, creating a large public greenspace. The park houses a wide variety of over 300 plant species, including perennials, bulbs, grasses, shrubs, and trees (a full list of species is available at the park's website, Plants of Lurie Garden, 2019). It is intensively maintained, with an approximate annual operating cost of $6 million (Farbstein, Axelrod, Shibley, & Wener, 2009). Millennium Park is a part of the larger Grant Park, a 1.29 km^2 park along the coast of Lake Michigan.

2.1.2. City Hall

The green roof installation on City Hall was completed in 2002 as a part of Chicago's Urban Heat Island (UHI) Initiative, which expressly aims to reduce the impacts of extreme heat in the city. The rooftop is 3600 m^2 with the garden covering about 1900 m^2 (Chicago City Hall, 2021). While the City Hall rooftop is the smallest of all sites examined, this intensive rooftop has a diverse ecosystem with over 150 plant species, including grasses, woody shrubs, and several trees - a cockspur hawthorne (*Crataegus crus-gally*) and a prairie crabapple (*Malus ioensis*) (City Hall's Rooftop Garden, 2021).

2.1.3. Walmart Supercenter

The Walmart Supercenter on 4650 W North Avenue was built in 2006, and the vegetation on its roof was installed at the time of building construction. The rooftop has an area of about 12,000 m^2, with the extensive green roof covering 7,000 m^2 and the rest being a high-albedo white surface. Only the green roof portion of the rooftop was analyzed in our study. The green roof is composed primarily of low-lying varieties of *Sedum*, *Dianthus*, and *Petrorhagia*, which are known for their drought tolerance and are commonly used on extensive green roofs. Irrigation was only used during the first growing season, and the plants did not grow in fully until 2009 (Green Roof Performance, 2013).

2.2. Data sources

To identify the rooftops with large surface areas and determine their boundaries for analysis, we draw on the City of Chicago's Green Roof Geodatabase, which was compiled in 2014. Constructed with high-resolution satellite imagery, the data include vector outlines of vegetated rooftops as well as the boundaries of vegetation within them. In some cases, such as Millennium Park, the vegetation boundaries outlined by the Green Roof Geodatabase include small, freestanding vegetated regions which we chose to exclude from our analysis. A schematic showing vegetated rooftop locations and their control sites is shown in Fig. 1.

We utilize the extensive longitudinal catalogue of Landsat 5 data to model LST and NDVI at each of our three green roof sites, plus a neighboring control site (unvegetated roof) matched to each treatment site. The modeling procedure used to estimate LST and NDVI is documented step-by-step in Appendix.

Landsat 5 is the best suited satellite mission for our purposes, as its temporal coverage allows us to evaluate years before and after green roof installation at each site. We draw on 60 Landsat 5 TM scenes, which we obtained from the U.S. Geological Survey's EarthExplorer website. We collected scenes that contain the City of Chicago, which are taken from paths 23 and 22, and row 31, and which are consistently

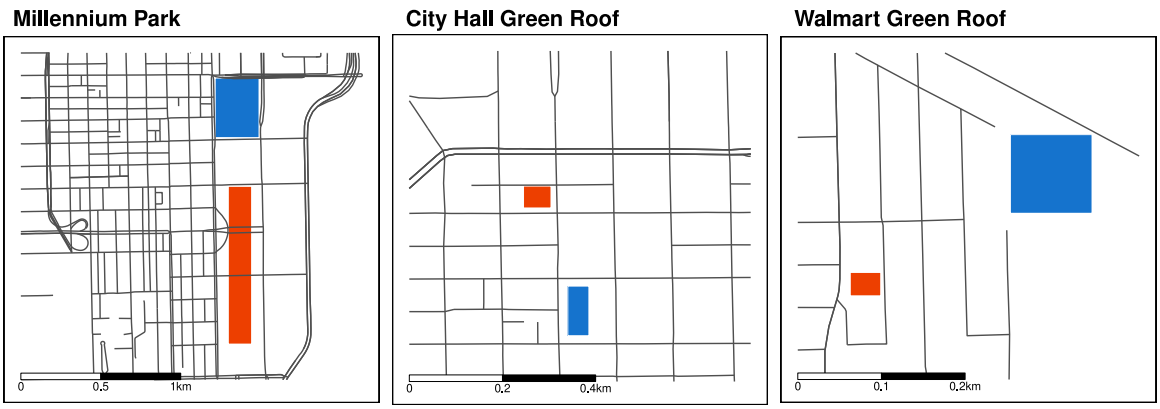

Fig. 1. The three vegetated rooftop sites studied in Chicago (shown in blue) and their neighboring control sites (shown in red). Boundaries shown are not exact. (For interpretation of the references to color in this figure legend, the reader is referred to the web version of this article.)

Table 1
Green roof analysis and Landsat 5 scene selection details.

Green roof site	Years of analysis	Installation years	Pre-Installation scenes	Post-Installation scenes
Millennium Park	1990–2011	1998–2004	15	23
Walmart	2000–2011	2005–2006	15	17
City Hall	1989–2011	2000–2002	22	33

collected between 11:16 and 11:22 AM Central Standard Time (GMT-6). Only scenes from the daytime during summer months (June, July, and August) that have less than 10% cloud cover were used. For each scene, we draw on band 6 (thermal infrared, 10.40-12.50 μ m), band 4 (near-infrared, 0.76-0.90 μ m), band 3 (red, 0.63-0.69 μ m), and the BQA (quality assurance) band, all of which are available at 30-meter resolution (U.S. Geological Survey, 2021).

Although LST differs from air temperature – which more directly affects humans' thermal comfort – it can be a valuable proxy for evaluating changes over time and identifying relative heat exposure risk between sites. In contrast to ground-based temperature measurements, satellite-based heat models can cover large spatial and temporal scopes at relatively low cost for the researcher. As a result, this approach is especially useful for capturing intra-urban temperature variation, longitudinal assessments, and analyses in resource-limited settings (Hu & Brunsell, 2015; Son, Chen, Chen, Thanh, & Vuong, 2017).

2.3. Identifying the causal effects of Green roof installation on LST and NDVI

After modeling LST and NDVI for each available Landsat 5 scene, the mean LST and NDVI values are extracted for each of the three rooftops. Each rooftop-wide mean extracted for a given date is then considered as a sample observation point. We next adopt a quasi-experimental framework to identify the causal effects of roof installation on LST and NDVI. Referred to as difference-in-differences analysis by social scientists (Angrist & Pischke, 2008; Imbens & Wooldridge, 2009) and before–after control-impact (BACI) design by physical scientists (Parison et al., 2020; Smith, 2002), this approach utilizes longitudinal data and linear mixed models to compare changes over time between treatment and control groups. We estimate the following model:

$$Y_t = \beta_0 + \beta_1 P_t + \beta_2 G_t + \beta_3 (P_t \cdot G_t) + \varepsilon_t \quad (1)$$

Where Y_t is the LST or NDVI outcome; P_t is a temporal indicator where 0 is pre-treatment and 1 is post-treatment; G_t indicates the treatment status of the site, 1 for green roof location and 0 for a neighboring control location; the β_3 coefficient on the interaction term $P_t \cdot G_t$ is the difference-in-differences estimator of interest, which measures the average treatment effect of green roof installation on LST and NDVI. For example, a negative β_3 value would indicate that the green roof had lower LST or NDVI values relative to its control site. ε_t represents residual errors. We include year fixed effects to control for any background temporal trends which may influence outcome variables across all sites, and estimate clustered standard errors.

In addition to the difference-in-differences analysis, which identifies relative changes in LST and NDVI between treatment and control sites, we use a nonparametric bootstrap to estimate pre- and post-installation LST values for each treatment and control site (Hall & Hart, 1990). This allows us to evaluate the absolute changes in LST over time across all sites.

2.4. Control site selection

We identified a control site for each of our three green roofs, selecting similarly sized rooftops with comparable elevations and within a 90–270 meter buffer of the matched green roof. The buffer was created to identify control sites that were near enough to experience comparable environmental conditions as the treatment site, but far enough so as not to experience spatial spillover effects from the green roof's vegetation (Parison et al., 2020). Such "oasis effects" are well-documented in the literature (Doick, Peace, & Hutchings, 2014; Shashua-Bar, Pearlmutter, & Erell, 2009; Sugawara et al., 2016), and care needs to be taken to select paired controls that are in this buffer. This step is critical for ensuring that the noninterference assumption in our statistical models – which asserts that the green roof treatment does not affect the control site – is upheld.

Since Millennium Park was constructed atop a railyard, the nearby exposed rail lines were used as the control area. Roughly 49,000 square meters of railroad were selected to serve as the control. Importantly, these sections of railroad are a similar distance from Lake Michigan as Millennium Park and are within the same local context, with dense urban development to their west and open green space to their east. For City Hall, the nearby 200 North LaSalle building was chosen to serve as the control site. This 30 floor building is about 200 meters from City Hall and was constructed in 1984 without incorporating green infrastructure on its rooftop. The control site selected for the Walmart site was an auto body shop about 175 meters away. This building was constructed in 1930 and has no observable green infrastructure.

Google Earth Pro was used to view historical aerial imagery for each of these control sites, ensuring there was no major construction at the

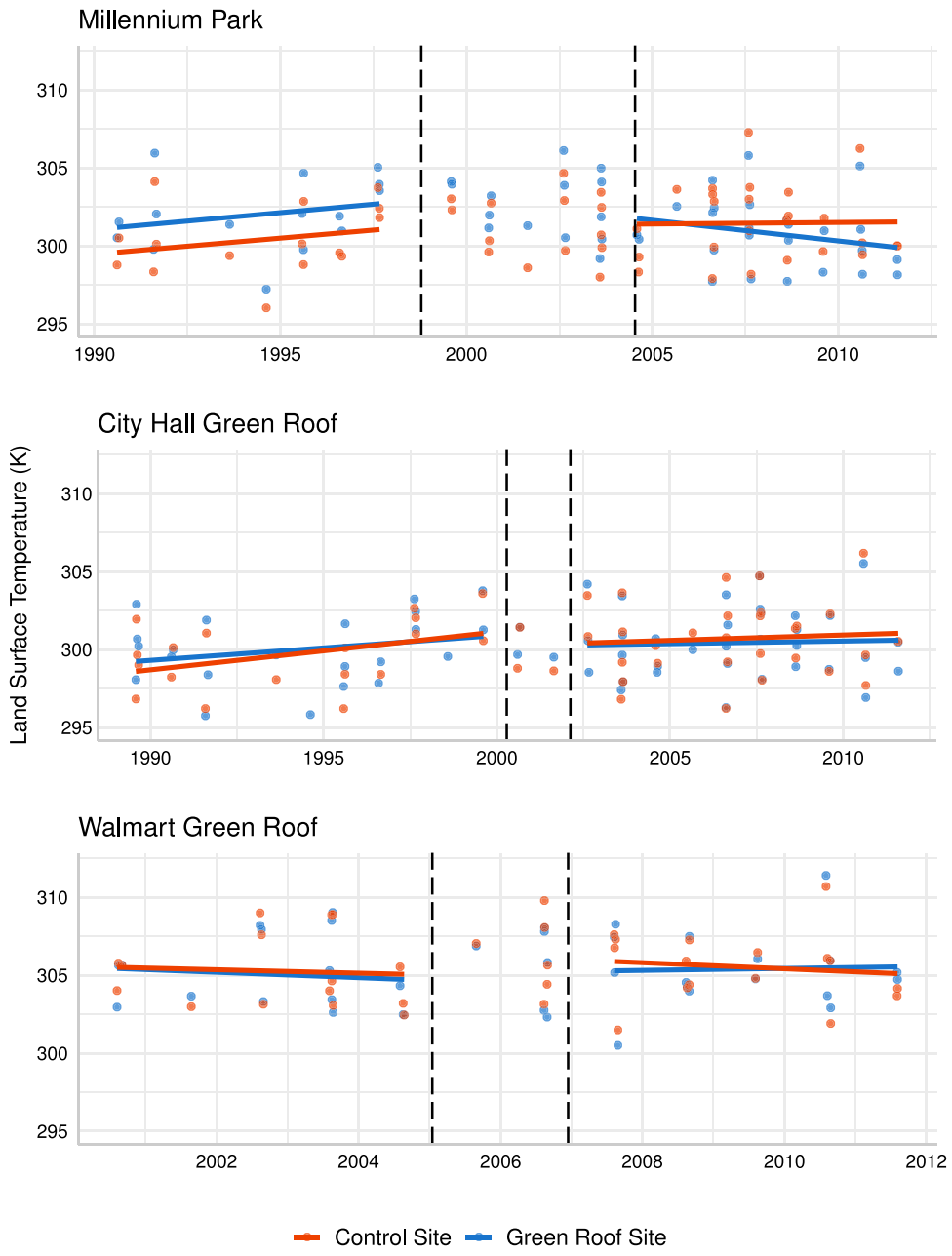

Fig. 2. Parallel trends plots for land surface temperature estimates. Vertical lines indicate green roof construction period. (For interpretation of the references to color in this figure legend, the reader is referred to the web version of this article.)

sites during our study period. We present parallel trends plots for each of the three matched sites to ensure that the selected control was appropriate for each treatment site. The presence of parallel curves prior to green roof installation (shown in Fig. 2) indicates that treatment and control sites respond similarly to broader environmental conditions and are an appropriate match.

3. Results

3.1. Descriptive results

We first present descriptive density plots illustrating the distribution of pre- and post-installation mean LST values for each green roof site and its control roof (shown in Fig. 3). These results show the largest change in distributions at Millennium Park. While this green roof had a higher mean LST as well as higher extreme values relative to its neighboring roof in the period prior to green roof installation, the trend switched after the green roof was established. In the post-installation period, Millennium Park had both a lower mean LST as well as fewer extreme values than its control roof.

The City Hall and Walmart rooftops show less dramatic changes. While the City Hall rooftop distribution shows more density at higher temperature values compared to its control site in the pre-installation period, this trend likewise changes in the post-installation period, although to a lesser degree than Millenium Park. However, the mean LST in the post-installation period for the green roof alone is still slightly higher when compared only to itself. The Walmart rooftop shows no change in the relationship between the green roof and its control site mean; in both periods the distribution center for the green roof is very slightly less than the center at the control site.

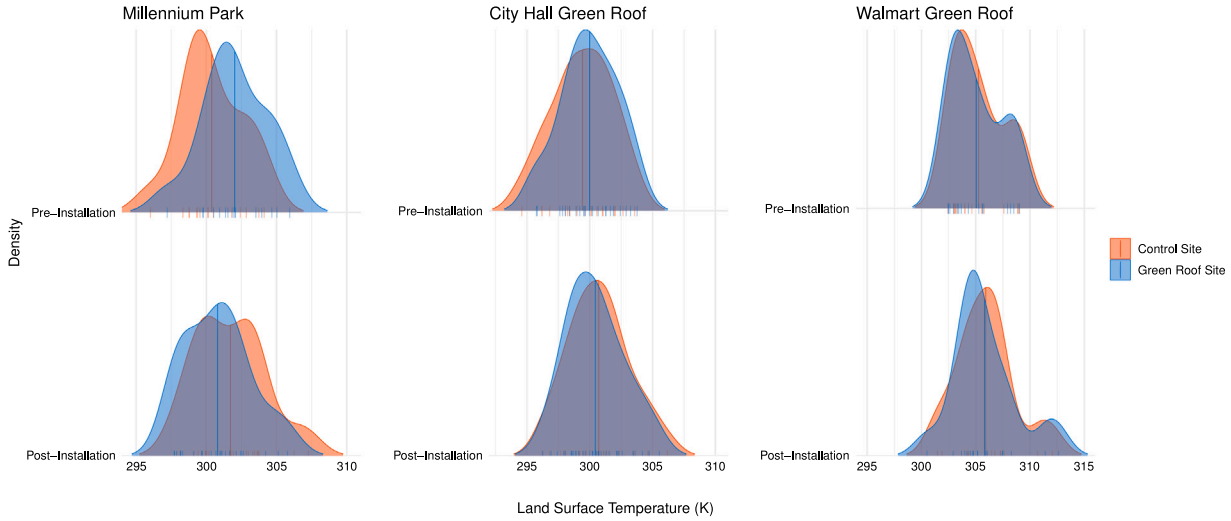

Fig. 3. Density plots of mean land surface temperature at each green roof and paired control site. Vertical lines indicate mean values.

3.2. Regression results

We next test changes in LST and NDVI in a difference-in-differences regression framework (reported in Table 2). Compared to the descriptive results reported above, this approach allows us to account for annual variability through the use of yearly fixed effects. Additionally, bootstrapped estimates allow us to evaluate absolute change in mean LST (shown in Fig. 4).

3.2.1. Millennium Park

Millennium Park experienced significantly lower LST (−2.55 K) along with a larger magnitude of NDVI (+0.16) in the post-installation period relative to its control site. Out of all three sites, Millennium Park was the only site at which absolute mean LST was lower in the post-installation period, indicating that the installation was able to fully mitigate larger warming trends.

3.3. City Hall

Like Millennium Park, the City Hall site also experienced significantly greater NDVI (+.15) and lower LST (-.98 K) in the post-installation period compared to its control site. However unlike Millennium Park, both the City Hall green roof and its control site experienced overall increases in mean LST in the post-installation period. In this case, while the green roof did have a significant heat reduction effect, it was not enough to lower LST in absolute terms.

3.4. Walmart Supercenter

Unlike Millennium Park and City Hall, the Walmart green roof was not constructed on an existing building, but rather was installed as a part of new building construction. For this site, the pre-installation treatment site was an empty, somewhat vegetated field, which was converted to a green roof on a new building in the post-installation period. This scenario allows us to test whether the green roof is able to mitigate the known warming effects of building densification (Guo et al., 2015).

The Walmart green roof experienced significantly lower NDVI (-.07) in the post-installation period relative to its control site. Examining the distribution of NDVI values, it is clear that the site's absolute NDVI level also declined in the post-installation period (see Appendix Fig. 1 for parallel trends plot of NDVI values), rebounding slightly in the years following construction. The treatment site also experienced a larger post-installation increase in LST (+0.12 K) relative to its neighboring control site, and both treated and control rooftops experienced absolute increases in LST in the post-construction period. In short, the green roof alone was not sufficient to mitigate the combined background warming trend and increased temperatures associated with building construction. In fact, the green roof performs largely the same as its unvegetated control site.

4. Discussion

Our findings suggest that there is significant variation in cooling performance across different green roof types and further suggests that not all green roofs can fully mitigate warming trends associated with climate change and urban densification. While Millennium Park showed the strongest heat mitigation performance with both absolute reductions in LST and relative reductions to its control site, the vegetated rooftop at City Hall showed only reductions in LST relative to its control site, but not in absolute terms. In short, Millennium Park was able to actively reduce urban heat, while City Hall was only able to partially mitigate larger warming trends. At the Walmart Supercenter green roof, NDVI levels after construction remained lower than the field which the building was constructed on, and the green roof and its control site experienced very similar LST levels in the post-installation period. This finding suggests that this particular type of extensive green roof may not be able to replace open greenspace in terms of its heat mitigation capacity. Further research focused on extensive rooftop performance is needed to thoroughly evaluate whether this green roof type is broadly limited in its cooling capacity and, if so, whether this is the case across differing climatic regions.

What might account for this variation in outcomes across different sites? We discuss several factors that may play a role in observed differences: plant type, rooftop location, rooftop structure, and indoor energy consumption.

Though often collapsed into the single catch-all term "green roof", existing literature suggests that there are important differences in vegetated rooftop types (Eksi, Rowe, Wichman, & Andresen, 2017). For example, of only a small number of studies that specifically compares green roof plant types, Lee, Ryu, and Jiang (2015) found that grass and *Sedum* rooftops had different effects on temperature (Lee et al., 2015). Such differences may be in part due to variation in plants' Leaf Area Index, which has been demonstrated to influence vegetation's cooling capacity (Hodo-Abalo, Banna, & Zeghmati, 2012). Millennium Park and City Hall can be considered "intensive" green roofs; they include vegetation of various size and genus, as well as shrubs and trees. In contrast, the Walmart green roof is considered an "extensive"

Table 2
Difference-in-differences regression results show the causal effects of green roof installation on land surface temperature (LST) and normalized difference vegetation index (NDVI) at each of the three study sites. The interaction term is the primary coefficient of interest, showing the change in LST or NDVI at the green roof site, relative to a neighboring control roof.

	Millennium Park		City Hall		Walmart	
	LST	NDVI	LST	NDVI	LST	NDVI
Constant	299.52***	0.13	299.55***	−0.07	305.06***	0.01
	(0.12)	(0.02)	(0.18)	(0.01)	(0.09)	(0.01)
Green Roof Site	1.63***	0.06***	0.72*	−0.01**	−0.22***	0.12***
	(0.00)	(0.00)	(0.03)	(0.00)	(0.00)	(0.00)
Post-Installation Period	0.26	−0.06	1.11	0.03	0.51*	0.02
	(0.10)	(0.03)	(0.60)	(0.01)	(0.03)	(0.02)
Green Roof * Post-Installation	−2.55***	0.16**	−0.98**	0.15**	0.12***	−0.07***
	(0.00)	(0.00)	(0.01)	(0.00)	(0.00)	(0.00)

*$p < 0.05$.
**$p < 0.01$.
***$p < 0.001$.

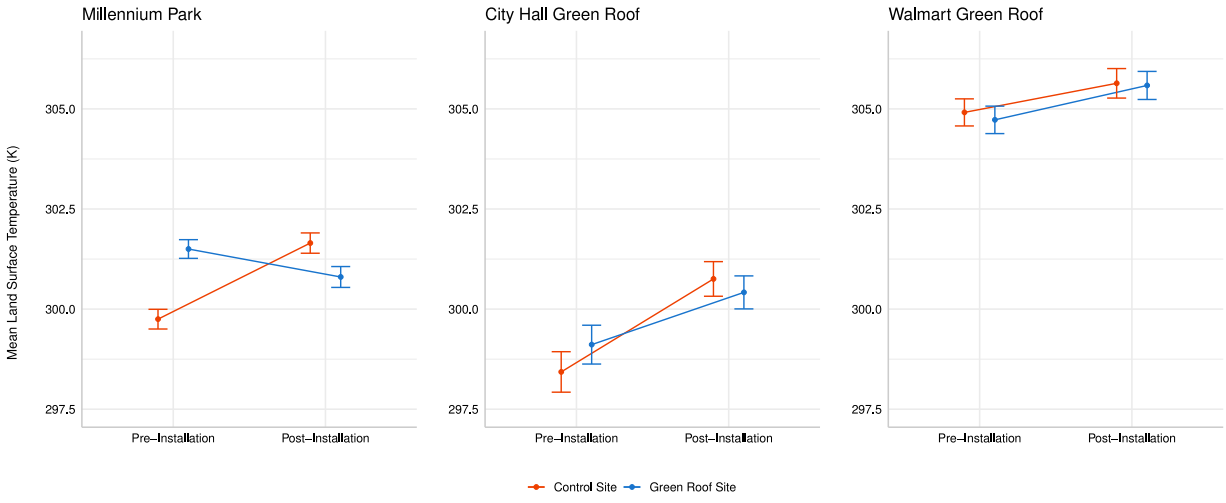

Fig. 4. Bootstrapped estimates for absolute change in LST between pre- and post-installation periods. Error bars indicate the 95% CI.

green roof; it is composed of single-genus *Sedum* plants that are both lightweight and lower in height. Our findings suggest that, in temperate regions such as Chicago, intensive green roofs may have stronger heat mitigation capacity than extensive green roofs. This conclusion concurs with findings from one of the few other studies to directly compare the two green roof types, which found that intensive roofs in Adelaide, Australia were cooler during the daytime than extensive roofs (Razzaghmanesh, Beecham, & Salemi, 2016).

In addition to the biophysical composition of a vegetated rooftop, the location of the roof itself may play a role in whether or not introduced vegetation can mitigate land surface temperature. Coseo and Larsen (2014) report a number of site-specific factors that can affect heat at a particular location, including proximity to car traffic, intensely developed areas, and water bodies, as well as surrounding building height, street width, and street direction (Coseo & Larsen, 2014). In Chicago, the eastern edge of the city directly abuts Lake Michigan, which has been found to have a cooling effect on adjacent neighborhoods (Ackerman, 1985). This finding is especially relevant to the Millennium Park site, which is located only a block away from Lake Michigan's edge.

Further, the structure of the rooftop itself may also play a role in determining whether or not a given green roof has the capacity to mitigate urban heat. While the Walmart Supercenter rooftop and Millennium Park are some of the largest green roofs in all of Chicago, the City Hall site is much smaller. This difference may explain why the City Hall green roof did not experience an absolute reduction in land surface temperature, despite having similar vegetation composition as Millennium Park, for which absolute reductions in land surface temperature were observed. Further, heat mitigation performance may be influenced by each rooftop's structure and thickness, including factors such as growing layer material composition, growing layer height, and presence of a drainage layer (Scharf & Zluwa, 2017).

Finally, energy consumption levels within each building may further influence each green roof's cooling capacity. For example, the amount of waste heat produced from air conditioning units operated within each building would likely influence localized heat conditions (Coseo & Larsen, 2014). Given the high cooling requirements for buildings that store perishable foods, we would expect waste heat levels to be higher at the Walmart site than at other sites examined. This may in part explain why no cooling effect was observed at the Walmart rooftop, although we note with caution that the results presented here cannot definitely explain the causal mechanisms operating behind the observed differences in rooftop cooling effects. Nevertheless, the study design presented offers a clear technique for future research to systematically evaluate the relative influence of the many factors listed above – vegetation type, rooftop location, waste heat production, rooftop structure, etc. – on green roof heat mitigation performance.

While our quasi-experimental research design is a more robust approach than the single image comparisons commonly used in remote sensing-based UHI research, our study nevertheless has limitations. By using satellite imagery, we are able to analyze a long temporal period and spatial scope, yet Landsat's 16-day temporal resolution and the occasional cloud cover means that we have smaller sample sizes than what would be ideal for statistical analysis.

A further limitation to our approach is the relatively coarse spatial resolution of the Landsat imagery we utilized (30 m x 30 m). While we prioritized using publicly available data to demonstrate the low-cost applicability of remote sensing analyses for green infrastructure policy evaluation, we acknowledge that this spatial scale is not perfectly able to capture fine spatial details. As a result, the data we utilized includes a small number of "mixed pixels", which collapse multiple land use types into a single pixel value, and which may include surfaces other than the green roof or control surface utilized in this study. This is especially likely at the City Hall site, where the tall height of the building means that imagery taken at an oblique angle may not exactly line up with the ground-level building footprint. Resulting mixed pixels may introduce a level of bias into our estimates, leading to an underestimation of a roof's cooling effect. However, because we observe post-installation changes in NDVI that would be expected from green roof installation (see Appendix Fig. A.1), we believe that the analysis procedure performs well enough to make causal inferences. Private satellite companies are increasingly making high-resolution imagery available – at a cost – for analysis. Future research should draw on these data to conduct more precise evaluations of green infrastructure, which may better avoid concerns over mixed pixels.

5. Conclusions

Our research moves beyond the general policy directive that green roofs are an effective urban heat mitigation strategy by demonstrating a methodology that can assess which types of green roofs cool most effectively and whether various green roof types can fully counteract background warming trends. Results from the three sites studied suggest that, in temperate regions such as the City of Chicago, intensive green roofs with heterogeneous plant types may have a superior capacity to mitigate urban heat than extensive, mono-species green roofs. In fact, the extensive green roof examined here does not show any cooling benefits compared to a nearby, non-vegetated rooftop, calling into question whether this particular type of green roof should be promoted as a means of heat reduction. This finding is in line with a small but growing number of studies that conclude that extensive or *Sedum*-based green roofs either have no effect on temperature (Yin, Kong, Dronova, Middel, & James, 2019) or, worse, actively increase temperature under some conditions (Solcerova, van de Ven, Wang, Rijsdijk, & van de Giesen, 2017; Zhang et al., 2020). As others have noted (Zheng et al., 2021), further research is needed to more thoroughly evaluate this possibility. The approach outlined in this study offers a means of doing so at low-cost, without the resource-intensive ground-based measurements that past work has relied upon.

Results from across the three sites also suggest that not all green roofs can fully counteract the larger warming trends associated with climate change and urbanization. Only the largest of the green roofs investigated for this study was able to reduce land surface temperature in absolute terms, with another only tempering the rate of temperature increase and a third resulting in no heat mitigation at all. These findings suggest that green roofs may not be the panacea for urban heat that some might hope, and that, as scholars have already pointed out, there are limits to current adaptation strategies (Dow et al., 2013).

This ability to distinguish between absolute temperature reduction from relative temperature mitigation is an important benefit to our study design. When evaluating green roof cooling performance over a multi-year temporal period, it is critical to be able to identify green roof-driven cooling trends amidst larger warming trends as well as from expected sampling variability embedded in the collected data. Integrating a comparative control site for each experimental green roof allows us to do so.

By drawing on robust, quasi-experimental analysis, publicly available satellite imagery, and open-source software, we demonstrate a low-cost evaluation method that can be adopted by planners and policymakers to assess the heat mitigation performance of green roofs in their own cities and towns. Developing such techniques that can quantify the cooling effects of green roofs is critical for practitioners who must balance the relative costs and benefits of green roof installation when making planning decisions (Teotónio, Silva, & Cruz, 2021). Further scholarly research on green roofs should aim to disentangle the relative influence of extensive versus intensive rooftop structure, rooftop size, and site location on the effectiveness of a roof's heat mitigation performance. Additionally, more evaluations of green roofs across different climatic zones are needed. It is well established that green infrastructure performs differently across geographic regions (Krayenhoff et al., 2018), and that climate adaptation projects in the Global South – in particular small- and mid-sized cities in Africa and Asia – are under researched (Lamb, Creutzig, Callaghan, & Minx, 2019). Further work is needed not only to more firmly describe which types of green roofs most effectively reduce heat, but whether various green roof types may perform differently across climatic regions (temperate, arid, tropical, etc.). The global coverage of public satellite imagery combined with the analytical methods proposed in this study make performing such evaluations at sites around the world feasible with far fewer resources than historically required for such research.

Declaration of competing interest

The authors declare that they have no known competing financial interests or personal relationships that could have appeared to influence the work reported in this paper.

Acknowledgments

Support was provided by the National Aeronautics and Space Administration's (NASA) Earth Science Division and NASA Goddard Institute for Space Studies through the NASA-Microsoft partnership and Climate Change Research Initiative (CCRI) respectively. Additional support was provided by the Peter J. Eloranta Summer Undergraduate Research Fellowship at MIT's Undergraduate Research Opportunities Program (UROP) and the Jeffrey L. Pressman Award from MIT's Department of Political Science. We thank the City of Chicago's Department of Planning and Development for providing data from the City of Chicago Green Roof Database and Raed Mansour at the Chicago Department of Public Health for his comments. Special thanks to Matthew Pearce and Rosalba Giarratano for their programmatic support which made this research possible, and to Dr. Karen Seto for providing feedback on the manuscript.

Appendix

Land surface temperature modeling procedure

For each Landsat scene, we apply the following procedures (outlined in Appendix Fig. A.2) using R statistical software. First, we crop each Landsat raster such that it only includes cells within the City of Chicago. Next, we use the BQA band to mask out cells that do not include cloud cover (specifically, for cell values equal to 672).

After these pre-processing steps, we convert the cells in band 6 from digital numbers to radiance using the following equation:

$$L_\lambda = M_L Q_C + A_L \tag{2}$$

Where L_λ is Top of Atmosphere (TOA) spectral radiance, M_L is the band-specific multiplicative rescaling factor from the metadata, Q_C is the Band 6 image (raster), and A_L is the band-specific additive rescaling factor from the metadata.

The radiance of band 6 is then converted to brightness temperature from the following equation:

$$BT = \frac{K_2}{ln(\frac{K_1}{L_\lambda} + 1)} \tag{3}$$

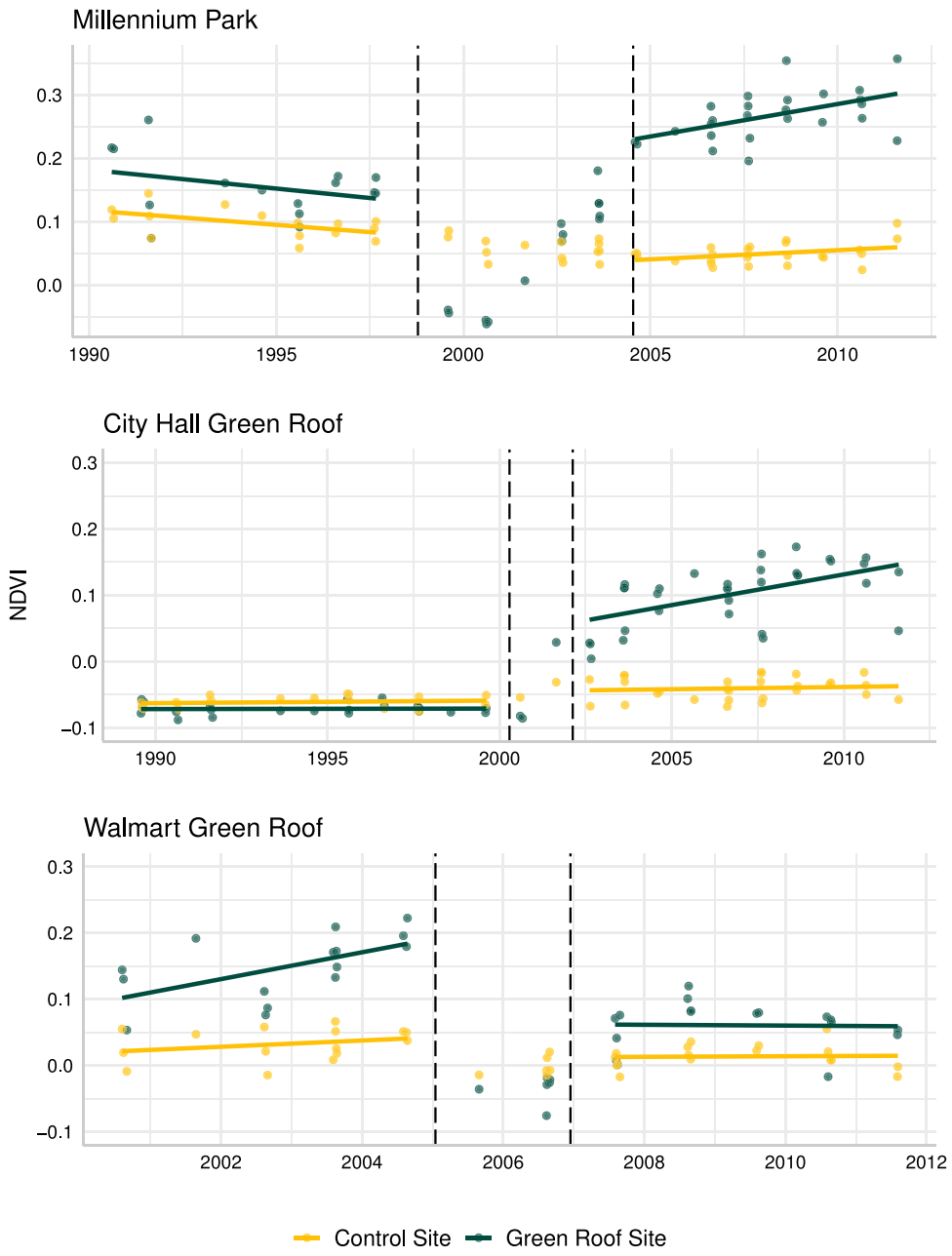

Fig. A.1. Parallel trends plots for Normalized Difference Vegetation Index (NDVI) estimates. Vertical lines indicate green roof construction period. (For interpretation of the references to color in this figure legend, the reader is referred to the web version of this article.)

Where BT is the brightness temperature, K_1 is the band-specific thermal conversion constant taken from metadata and K_2 is the band-specific thermal conversion constant taken from metadata.

After calculating the brightness temperature from band 6, we use bands 3 and 4 to model emissivity, which measures the extent to which a given material emits thermal radiation. Different land cover types have different emissivity, which in turn affect how temperature is modeled. While it is recognized that emissivity is an important component of land surface temperature modeling, many models often assume constant emissivity across a landscape (Al-Hamdan, Quattrochi, Bounoua, Lachir, & Zhang, 2016). We can improve our estimates of land surface temperature by incorporating location (point) specific emissivity. One approach for estimating emissivity is by calculating the "vegetation fraction". To calculate emissivity in this way, we use the methodology detailed below (Son et al., 2017).

First, the normalized difference vegetation index (NDVI) is calculated. NDVI is a vegetation index that estimates how much biomass exists within a given pixel, and is scaled from −1 (water) to +1 (dense vegetation). NDVI values approaching zero correspond to barren areas of sand or rock. NDVI is calculated as follows:

$$NDVI = \frac{NIR - R}{NIR + R} \tag{4}$$

Where NIR is the near-infrared energy associated with band 4 of Landsat 5, and R corresponds to "red" energy measurements associated with band 3 of Landsat 5. $NDVI$ is then converted to vegetation fraction using the following equation:

$$P_v = \left(\frac{NDVI - NDVI_{min}}{NDVI_{max} - NDVI_{min}}\right)^2 \tag{5}$$

Where P_v refers to the vegetation fraction, and $NDVI$ minimum ($NDVI_{min}$) and maximum ($NDVI_{max}$) values are taken from the individual Landsat scene within the Chicago boundary. Vegetation fraction

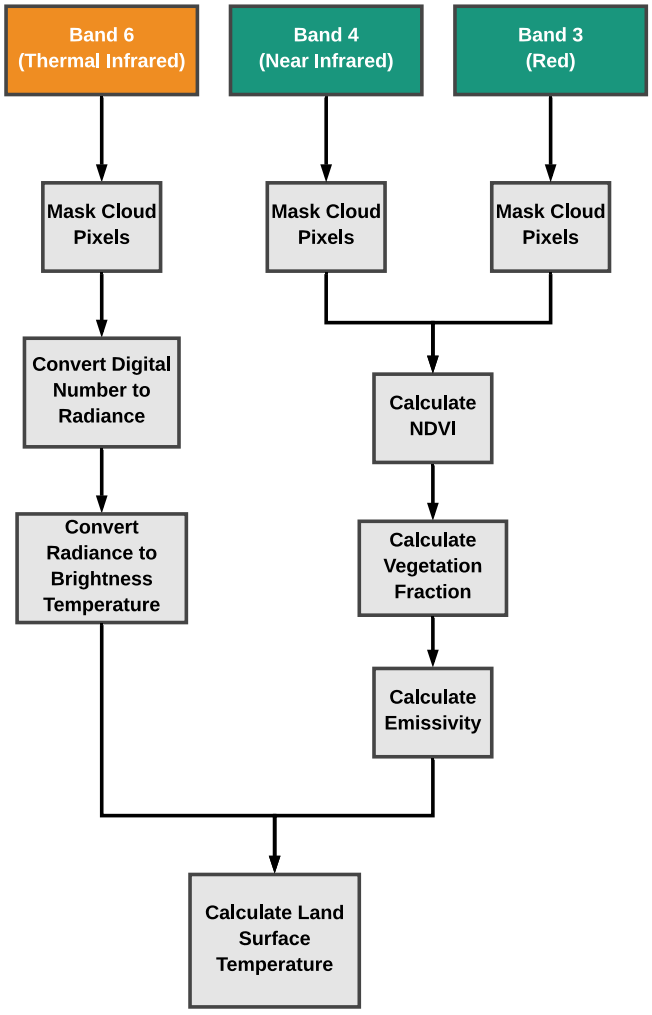

Fig. A.2. Landsat 5 Land Surface Temperature modeling procedure.

is then converted to emissivity as follows:

$$\varepsilon_{TM} = 0.004 P_v + 0.986481 \tag{6}$$

Finally, LST is calculated with the following equation:

$$LST = \frac{BT}{1 + w\frac{BT}{Q} ln(\varepsilon)} \tag{7}$$

In the equation above, BT refers to brightness temperature, w refers to the wavelength for the thermal band in use, and ε refers to emissivity. Additionally, Q, the second radiation constant, is calculated through the following equation: $Q = \frac{hc}{s} = 1.438 \cdot 10^{-2}$ m K, where h is Planck's constant, c is the speed of light, and s is Boltzmann's constant. Final LST and NDVI models for the City of Chicago are shown in Fig. A.3.

References

Ackerman, B. (1985). Temporal march of the Chicago heat island. *Journal of Climate and Applied Meteorology*, *24*(6), 547–554, URL https://journals.ametsoc.org/doi/abs/10.1175/1520-0450(1985)024%3C0547:TMOTCH%3E2.0.CO%3B2.

Al-Hamdan, M. Z., Quattrochi, D. A., Bounoua, L., Lachir, A., & Zhang, P. (2016). Using landsat, MODIS, and a biophysical model to evaluate LST in urban centers. *Remote Sensing*, *8*(11), 952, URL https://www.mdpi.com/2072-4292/8/11/952.

Allen, L., Lindberg, F., & Grimmond, C. S. B. (2011). Global to city scale urban anthropogenic heat flux: model and variability. *International Journal of Climatology*, *31*(13), 1990–2005, URL https://rmets.onlinelibrary.wiley.com/doi/abs/10.1002/joc.2210.

Angrist, J. D., & Pischke, J.-S. (2008). *Mostly Harmless Econometrics: an Empiricist's Companion*. Princeton, NJ: Princeton University Press, Google-Books-ID, ztXL21Xd8v8C.

Aylett, A. (2015). Institutionalizing the urban governance of climate change adaptation: Results of an international survey. *Urban Climate*, *14*, 4–16, URL https://linkinghub.elsevier.com/retrieve/pii/S2212095515300031.

Bartesaghi Koc, C., Osmond, P., & Peters, A. (2018). Evaluating the cooling effects of green infrastructure: A systematic review of methods, indicators and data sources. *Solar Energy*, *166*, 486–508, URL http://www.sciencedirect.com/science/article/pii/S0038092X18302172.

Basu, R. (2009). High ambient temperature and mortality: a review of epidemiologic studies from 2001 to 2008. *Environmental Health*, *8*(1), 40, URL https://doi.org/10.1186/1476-069X-8-40.

Berardi, U. (2016). The outdoor microclimate benefits and energy saving resulting from green roofs retrofits. *Energy and Buildings*, *121*, 217–229, URL https://www.sciencedirect.com/science/article/pii/S037877881630158X.

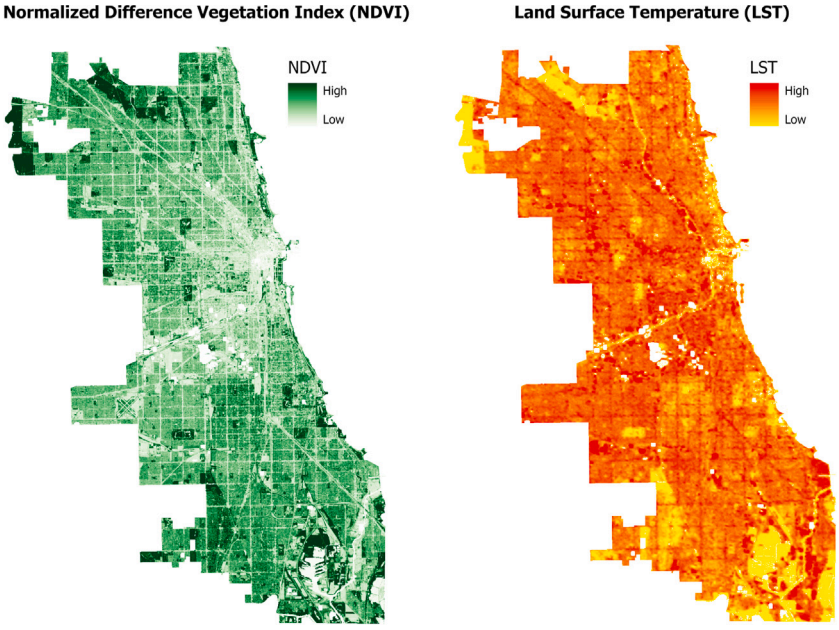

Fig. A.3. Landsat 5 (a) Normalized Difference Vegetation Index (NDVI) and (b) Land Surface Temperature (LST) models for the City of Chicago. Source: Landsat 5 TM, 8/24/2003, 11:12 AM CST.

Blanusa, T., Vaz Monteiro, M. M., Fantozzi, F., Vysini, E., Li, Y., & Cameron, R. W. F. (2013). Alternatives to Sedum on green roofs: Can broad leaf perennial plants offer better 'cooling service'? *Building and Environment*, *59*, 99–106, URL http://www.sciencedirect.com/science/article/pii/S0360132312002132.

Bowler, D. E., Buyung-Ali, L., Knight, T. M., & Pullin, A. S. (2010). Urban greening to cool towns and cities: A systematic review of the empirical evidence. *Landscape and Urban Planning*, *97*(3), 147–155, URL https://linkinghub.elsevier.com/retrieve/pii/S0169204610001234.

Chapman, S., Watson, J. E. M., Salazar, A., Thatcher, M., & McAlpine, C. A. (2017). The impact of urbanization and climate change on urban temperatures: a systematic review. *Landscape Ecology*, *32*(10), 1921–1935, URL https://doi.org/10.1007/s10980-017-0561-4.

Chen, X.-L., Zhao, H.-M., Li, P.-X., & Yin, Z.-Y. (2006). Remote sensing image-based analysis of the relationship between urban heat island and land use/cover changes. *Remote Sensing of Environment*, *104*(2), 133–146, URL https://www.sciencedirect.com/science/article/pii/S0034425706001787.

Chicago City Hall. (2021). URL https://www.greenroofs.com/projects/chicago-city-hall/.

Chicago Zoning Ordinance 17-4-1015 green roofs incentive. (2015). URL https://www.adaptationclearinghouse.org/resources/chicago-zoning-ordinance-17-4-1015-green-roofs-incentives.html.

Chin, G., Desjarlais, A., Estes, M., Hitchcock, D., Parker, D., Rosenthal, J., et al. (2008). *Reducing urban heat islands: Compendium of strategies*: *Technical report*, U.S. Environmental Protection Agency, URL https://www.epa.gov/sites/production/files/2017-05/documents/reducing_urban_heat_islands_ch_4.pdf.

City Hall's Rooftop Garden. (2021). URL https://www.chicago.gov/content/city/en/depts/dgs/supp_info/city_hall_green_roof.html.

Coseo, P., & Larsen, L. (2014). How factors of land use/land cover, building configuration, and adjacent heat sources and sinks explain Urban Heat Islands in Chicago. *Landscape and Urban Planning*, *125*, 117–129, URL http://www.sciencedirect.com/science/article/pii/S0169204614000607.

Dell, M., Jones, B. F., & Olken, B. A. (2012). Temperature shocks and economic growth: Evidence from the last half century. *American Economic Journal: Macroeconomics*, *4*(3), 66–95, URL https://www.aeaweb.org/articles?id=10.1257/mac.4.3.66.

Doick, K. J., Peace, A., & Hutchings, T. R. (2014). The role of one large greenspace in mitigating London's nocturnal urban heat island. *Science of the Total Environment*, *493*, 662–671, URL https://www.sciencedirect.com/science/article/pii/S0048969714009036.

Dong, J., Lin, M., Zuo, J., Lin, T., Liu, J., Sun, C., et al. (2020). Quantitative study on the cooling effect of green roofs in a high-density urban Area—A case study of Xiamen, China. *Journal of Cleaner Production*, *255*, Article 120152, URL https://www.sciencedirect.com/science/article/pii/S0959652620301992.

Dosio, A., Mentaschi, L., Fischer, E. M., & Wyser, K. (2018). Extreme heat waves under 1.5° C and 2° C global warming. *Environmental Research Letters*, *13*(5), Article 054006, URL https://doi.org/10.1088%2F1748-9326%2Faab827.

Dow, K., Berkhout, F., Preston, B. L., Klein, R. J. T., Midgley, G., & Shaw, M. R. (2013). Limits to adaptation. *Nature Climate Change*, *3*(4), 305–307, URL https://www.nature.com/articles/nclimate1847.

Eksi, M., Rowe, D. B., Wichman, I. S., & Andresen, J. A. (2017). Effect of substrate depth, vegetation type, and season on green roof thermal properties. *Energy and Buildings*, *145*, 174–187, URL https://www.sciencedirect.com/science/article/pii/S0378778817312203.

Erdem Okumus, D., & Terzi, F. (2021). Evaluating the role of urban fabric on surface urban heat island: The case of Istanbul. *Sustainable Cities and Society*, *73*, Article 103128, URL https://www.sciencedirect.com/science/article/pii/S2210670721004108.

Farbstein, J., Axelrod, E., Shibley, R., & Wener, R. (2009). *2009 rudy bruner award: Silver medal winner, millenium park*: *Technical report*, Bruner Foundation, Inc., URL http://www.rudybruneraward.org/wp-content/uploads/2016/08/06-Millennium-Park.pdf.

Gill, S., Handley, J., Ennos, A., & Pauleit, S. (2007). Adapting cities for climate change: The role of the green infrastructure. *Built Environment*, *33*(1), 115–133.

Gohain, K. J., Mohammad, P., & Goswami, A. (2021). Assessing the impact of land use land cover changes on land surface temperature over Pune city, India. *Quaternary International*, *575–576*, 259–269, URL https://www.sciencedirect.com/science/article/pii/S1040618220302299.

Green roof performance: A cost-benefit analysis based on Walmart's Chicago store. (2013). URL http://cdn.corporate.walmart.com/95/ab/ecb63ba44f51bec6f9aa42c73a9e/walmart-2013-green-roof-report.pdf.

Guo, G., Wu, Z., Xiao, R., Chen, Y., Liu, X., & Zhang, X. (2015). Impacts of urban biophysical composition on land surface temperature in urban heat island clusters. *Landscape and Urban Planning*, *135*, 1–10, URL http://www.sciencedirect.com/science/article/pii/S0169204614002679.

Guo, A., Yang, J., Xiao, X., Xia (Cecilia), J., Jin, C., & Li, X. (2020). Influences of urban spatial form on urban heat island effects at the community level in China. *Sustainable Cities and Society*, *53*, Article 101972, URL https://www.sciencedirect.com/science/article/pii/S2210670719320062.

Habeeb, D., Vargo, J., & Stone, B. (2015). Rising heat wave trends in large US cities. *Natural Hazards*, *76*(3), 1651–1665, URL https://doi.org/10.1007/s11069-014-1563-z.

Halder, B., Bandyopadhyay, J., & Banik, P. (2021). Monitoring the effect of urban development on urban heat island based on remote sensing and geo-spatial approach in Kolkata and adjacent areas, India. *Sustainable Cities and Society*, *74*, Article 103186, URL https://www.sciencedirect.com/science/article/pii/S2210670721004649.

Hall, P., & Hart, J. D. (1990). Bootstrap test for difference between means in nonparametric regression. *Journal of the American Statistical Association*, *85*(412), 1039–1049, URL https://www.jstor.org/stable/2289600.

Hayhoe, K., Sheridan, S., Kalkstein, L., & Greene, S. (2010). Climate change, heat waves, and mortality projections for chicago. *Journal of Great Lakes Research*, *36*, 65–73, URL http://www.sciencedirect.com/science/article/pii/S0380133009002275.

Heusinger, J., & Weber, S. (2017). Surface energy balance of an extensive green roof as quantified by full year eddy-covariance measurements. *Science of the Total Environment*, *577*, 220–230, URL https://www.sciencedirect.com/science/article/pii/S0048969716323567.

Hodo-Abalo, S., Banna, M., & Zeghmati, B. (2012). Performance analysis of a planted roof as a passive cooling technique in hot-humid tropics. *Renewable Energy*, *39*(1), 140–148, URL http://www.sciencedirect.com/science/article/pii/S0960148111004125.

Hoegh-Guldberg, O., Jacob, D., Taylor, M., Bindi, M., Brown, S., Camilloni, I., et al. (2018). Impacts of 1.5° C of global warming on natural and human systems. In *Global warming of 1.5° C. An IPCC special report on the impacts of global warming of 1.5° C above pre-industrial levels and related global greenhouse gas emission pathways, in the context of strengthening the global response to the threat of climate change, sustainable development, and efforts to eradicate poverty*.

Hu, L., & Brunsell, N. A. (2015). A new perspective to assess the urban heat island through remotely sensed atmospheric profiles. *Remote Sensing of Environment*, *158*, 393–406, URL http://www.sciencedirect.com/science/article/pii/S0034425714004325.

Hurwitz, M. M., Braneon, C., Kirschbaum, D. B., Mandarino, F., & Mansour, R. (2020). Earth observations inform cities' operations and planning. *Eos*, *101*, 28–33, URL https://epizodyspace.ru/bibl/inostr-yazyki/Eos_Earth_and_Space_Science_News/2020/9/Hurwitz_et_al_---_Cities_Operations_and_Planning_Eos_101_no_09_(2020).pdf.

Imbens, G. W., & Wooldridge, J. M. (2009). Recent developments in the econometrics of program evaluation. *Journal of Economic Literature*, *47*(1), 5–86, URL https://www.aeaweb.org/articles?id=10.1257/jel.47.1.5.

Jiang, S., Lee, X., Wang, J., & Wang, K. (2019). Amplified urban heat islands during heat wave periods. *Journal of Geophysical Research: Atmospheres*, *124*(14), 7797–7812, URL https://agupubs.onlinelibrary.wiley.com/doi/abs/10.1029/2018JD030230.

Kazmierczak, A., & Carter, J. (2010). *Adaptation to climate change using green and blue infrastructure A database of case studies*: *Technical report*, Manchester, UK: University of Manchester.

Klinenberg, E. (2015). *Heat wave: A social autopsy of disaster in Chicago*. University of Chicago Press.

Krayenhoff, E. S., Moustaoui, M., Broadbent, A. M., Gupta, V., & Georgescu, M. (2018). Diurnal interaction between urban expansion, climate change and adaptation in US cities. *Nature Climate Change*, *8*(12), 1097–1103, URL http://www.nature.com/articles/s41558-018-0320-9.

Lamb, W. F., Creutzig, F., Callaghan, M. W., & Minx, J. C. (2019). Learning about urban climate solutions from case studies. *Nature Climate Change*, *9*(4), 279–287, URL https://www.nature.com/articles/s41558-019-0440-x.

Lee, S., Ryu, Y., & Jiang, C. (2015). Urban heat mitigation by roof surface materials during the East Asian summer monsoon. *Environmental Research Letters*, *10*(12), Article 124012, URL http://stacks.iop.org/1748-9326/10/i=12/a=124012?key=crossref.7d8341172cdf5f57402a9066f330abcd.

Li, Z.-L., Tang, B.-H., Wu, H., Ren, H., Yan, G., Wan, Z., et al. (2013). Satellite-derived land surface temperature: Current status and perspectives. *Remote Sensing of Environment*, *131*, 14–37, URL http://www.sciencedirect.com/science/article/pii/S0034425712004749.

Liu, J., Zhang, L., Zhang, Q., Zhang, G., & Teng, J. (2021). Predicting the surface urban heat island intensity of future urban green space development using a multi-scenario simulation. *Sustainable Cities and Society*, *66*, Article 102698, URL https://www.sciencedirect.com/science/article/pii/S2210670720309124.

MacIvor, J. S., & Lundholm, J. (2011). Performance evaluation of native plants suited to extensive green roof conditions in a maritime climate. *Ecological Engineering*, *37*(3), 407–417, URL http://www.sciencedirect.com/science/article/pii/S0925857410002910.

Mackey, C. W., Lee, X., & Smith, R. B. (2012). Remotely sensing the cooling effects of city scale efforts to reduce urban heat island. *Building and Environment*, *49*, 348–358, URL http://www.sciencedirect.com/science/article/pii/S0360132311002472.

Mahdiyar, A., Tabatabaee, S., Abdullah, A., & Marto, A. (2018). Identifying and assessing the critical criteria affecting decision-making for green roof type selection. *Sustainable Cities and Society*, *39*, 772–783, URL http://www.sciencedirect.com/science/article/pii/S2210670717317237.

Mallen, E., Bakin, J., Stone, B., Sivakumar, R., & Lanza, K. (2020). Thermal impacts of built and vegetated environments on local microclimates in an Urban University campus. *Urban Climate*, *32*, Article 100640, URL https://www.sciencedirect.com/science/article/pii/S2212095519301853.

Meehl, G. A., & Tebaldi, C. (2004). More intense, more frequent, and longer lasting heat waves in the 21st century. *Science*, *305*(5686), 994–997, URL https://science.sciencemag.org/content/305/5686/994.

Mohajerani, A., Bakaric, J., & Jeffrey-Bailey, T. (2017). The urban heat island effect, its causes, and mitigation, with reference to the thermal properties of asphalt concrete. *Journal of Environmental Management*, *197*, 522–538, URL http://www.sciencedirect.com/science/article/pii/S0301479717303201.

Norton, B. A., Coutts, A. M., Livesley, S. J., Harris, R. J., Hunter, A. M., & Williams, N. S. G. (2015). Planning for cooler cities: A framework to prioritise green infrastructure to mitigate high temperatures in urban landscapes. *Landscape and Urban Planning*, *134*, 127–138, URL http://www.sciencedirect.com/science/article/pii/S0169204614002503.

Oberndorfer, E., Lundholm, J., Bass, B., Coffman, R. R., Doshi, H., Dunnett, N., et al. (2007). Green roofs as urban ecosystems: Ecological structures, functions, and services. *BioScience*, *57*(10), 823–833, URL https://academic.oup.com/bioscience/article/57/10/823/232363.

Oke, T. R. (1982). The energetic basis of the urban heat island. *Quarterly Journal of the Royal Meteorological Society*, *108*(455), 1–24, URL https://rmets.onlinelibrary.wiley.com/doi/abs/10.1002/qj.49710845502.

Oleson, K. (2012). Contrasts between urban and rural climate in CCSM4 CMIP5 climate change scenarios. *Journal of Climate*, *25*(5), 1390–1412, URL https://journals.ametsoc.org/view/journals/clim/25/5/jcli-d-11-00098.1.xml.

Oleson, K. W., Monaghan, A., Wilhelmi, O., Barlage, M., Brunsell, N., Feddema, J., et al. (2015). Interactions between urbanization, heat stress, and climate change. *Climatic Change*, *129*(3), 525–541, URL https://doi.org/10.1007/s10584-013-0936-8.

Parison, S., Hendel, M., & Royon, L. (2020). A statistical method for quantifying the field effects of urban heat island mitigation techniques. *Urban Climate*, *33*, Article 100651, URL http://www.sciencedirect.com/science/article/pii/S2212095519301713.

Plants of Lurie garden. (2019). URL https://www.luriegarden.org/plant-life/.

Razzaghmanesh, M., Beecham, S., & Salemi, T. (2016). The role of green roofs in mitigating urban heat island effects in the metropolitan area of adelaide, south Australia. *Urban Forestry & Urban Greening*, *15*, 89–102, URL https://linkinghub.elsevier.com/retrieve/pii/S1618866715001788.

Rizvi, S. H., Alam, K., & Iqbal, M. J. (2019). Spatio -temporal variations in urban heat island and its interaction with heat wave. *Journal of Atmospheric and Solar-Terrestrial Physics*, *185*, 50–57, URL https://www.sciencedirect.com/science/article/pii/S1364682618304012.

Santamouris, M. (2015). Regulating the damaged thermostat of the cities—Status, impacts and mitigation challenges. *Energy and Buildings*, *91*, 43–56, URL http://www.sciencedirect.com/science/article/pii/S037877881500033X.

Scharf, B., & Zluwa, I. (2017). Case study investigation of the building physical properties of seven different green roof systems. *Energy and Buildings*, *151*, 564–573, URL https://www.sciencedirect.com/science/article/pii/S0378778817320856.

Shafique, M., Kim, R., & Rafiq, M. (2018). Green roof benefits, opportunities and challenges – A review. *Renewable and Sustainable Energy Reviews*, *90*, 757–773, URL http://www.sciencedirect.com/science/article/pii/S136403211830217X.

Sharma, A., Conry, P., Fernando, H. J. S., Hamlet, A. F., Hellmann, J. J., & Chen, F. (2016). Green and cool roofs to mitigate urban heat island effects in the Chicago metropolitan area: evaluation with a regional climate model. *Environmental Research Letters*, *11*(6), Article 064004, URL: https://doi.org/10.1088%2F1748-9326%2F11%2F6%2F064004.

Shashua-Bar, L., Pearlmutter, D., & Erell, E. (2009). The cooling efficiency of urban landscape strategies in a hot dry climate. *Landscape and Urban Planning*, *92*(3), 179–186, URL https://www.sciencedirect.com/science/article/pii/S0169204609000723.

Smith, E. P. (2002). BACI design. In A. H. El-shaarawi, W. W. Piegorsch, & J. Wiley (Eds.), *Encyclopedia of environmetrics, vol. 1* (pp. 141–148). John Wiley & Sons.

Smith, K. R., & Roebber, P. J. (2011). Green roof mitigation potential for a proxy future climate scenario in Chicago, Illinois. *Journal of Applied Meteorology and Climatology*, *50*(3), 507–522, URL https://journals.ametsoc.org/doi/full/10.1175/2010JAMC2337.1.

Solcerova, A., van de Ven, F., Wang, M., Rijsdijk, M., & van de Giesen, N. (2017). Do green roofs cool the air? *Building and Environment*, *111*, 249–255, URL https://www.sciencedirect.com/science/article/pii/S036013231630422X.

Son, N.-T., Chen, C.-F., Chen, C.-R., Thanh, B.-X., & Vuong, T.-H. (2017). Assessment of urbanization and urban heat islands in Ho Chi Minh City, Vietnam using Landsat data. *Sustainable Cities and Society*, *30*, 150–161, URL http://www.sciencedirect.com/science/article/pii/S2210670716305807.

Sugawara, H., Shimizu, S., Takahashi, H., Hagiwara, S., Narita, K.-i., Mikami, T., et al. (2016). Thermal influence of a large green space on a hot urban environment. *Journal of Environmental Quality*, *45*(1), 125–133, URL https://acsess.onlinelibrary.wiley.com/doi/abs/10.2134/jeq2015.01.0049.

Teotónio, I., Silva, C. M., & Cruz, C. O. (2021). Economics of green roofs and green walls: A literature review. *Sustainable Cities and Society*, *69*, Article 102781, URL https://www.sciencedirect.com/science/article/pii/S2210670721000731.

Tewari, M., Yang, J., Kusaka, H., Salamanca, F., Watson, C., & Treinish, L. (2019). Interaction of urban heat islands and heat waves under current and future climate conditions and their mitigation using green and cool roofs in New York city and Phoenix, Arizona. *Environmental Research Letters*, *14*(3), Article 034002, URL https://doi.org/10.1088/1748-9326/aaf431.

Tian, P., Li, J., Cao, L., Pu, R., Wang, Z., Zhang, H., et al. (2021). Assessing spatiotemporal characteristics of urban heat islands from the perspective of an urban expansion and green infrastructure. *Sustainable Cities and Society*, *74*, Article 103208, URL https://www.sciencedirect.com/science/article/pii/S2210670721004868.

Urban Climate Change Research Network (2018). *Impact 2050: The future of cities under climate change*: *UCCRN Technical report*, UCCRN Technical Report, URL https://c40-production-images.s3.us-west-2.amazonaws.com/impact2050report.pdf.

U. S. Geological Survey (2021). *What are the band designations for the Landsat satellites?*: *Technical report*, U.S. Geological Survey, URL https://www.usgs.gov/faqs/what-are-band-designations-landsat-satellites?qt-news_science_products=0#qt-news_science_products.

Wilson, B., & Chakraborty, A. (2018). Mapping vulnerability to extreme heat events: lessons from metropolitan Chicago. *Journal of Environmental Planning and Management*, 1–24, URL https://doi.org/10.1080/09640568.2018.1462475.

Yin, H., Kong, F., Dronova, I., Middel, A., & James, P. (2019). Investigation of extensive green roof outdoor spatio-temporal thermal performance during summer in a subtropical monsoon climate. *Science of the Total Environment*, *696*, Article 133976, URL https://www.sciencedirect.com/science/article/pii/S0048969719339464.

Yuan, F., & Bauer, M. E. (2007). Comparison of impervious surface area and normalized difference vegetation index as indicators of surface urban heat island effects in Landsat imagery. *Remote Sensing of Environment*, *106*(3), 375–386, URL https://www.sciencedirect.com/science/article/pii/S0034425706003191.

Zhang, G., He, B.-J., & Dewancker, B. J. (2020). The maintenance of prefabricated green roofs for preserving cooling performance: A field measurement in the subtropical city of Hangzhou, China. *Sustainable Cities and Society*, *61*, Article 102314, URL https://www.sciencedirect.com/science/article/pii/S2210670720305357.

Zheng, X., Kong, F., Yin, H., Middel, A., Liu, H., Wang, D., et al. (2021). Outdoor thermal performance of green roofs across multiple time scales: A case study in subtropical China. *Sustainable Cities and Society*, *70*, Article 102909, URL https://www.sciencedirect.com/science/article/pii/S2210670721001979.